New Phytologist

Research

Scale dependence of canopy trait distributions along a tropical forest elevation gradient

Gregory P. Asner[1], Roberta E. Martin[1], Christopher B. Anderson[1], Katherine Kryston[1], Nicholas Vaughn[1], David E. Knapp[1], Lisa Patrick Bentley[2], Alexander Shenkin[2], Norma Salinas[2,3], Felipe Sinca[1], Raul Tupayachi[1], Katherine Quispe Huaypar[4], Milenka Montoya Pillco[4], Flor Delis Ccori Álvarez[4], Sandra Díaz[5], Brian J. Enquist[6,7] and Yadvinder Malhi[2]

[1]Department of Global Ecology, Carnegie Institution for Science, 260 Panama Street, Stanford, CA 94305, USA; [2]Environmental Change Institute, School of Geography and the Environment, University of Oxford, Oxford, OX1 3QY, UK; [3]Sección Química, Pontificia Universidad Católica del Perú, Avenida Universitaria 1801, San Miguel, Lima32, Perú; [4]Universidad Nacional de San Antonio Abad del Cusco, Av. de la Cultura, Nro. 733, Cusco, Perú; [5]Instituto Multidisciplinario de Biología Vegetal (IMBIV), CONICET and FCEFyN, Universidad Nacional de Córdoba, Casilla de Correo 495, 5000 Córdoba, Argentina; [6]Department of Ecology and Evolutionary Biology, University of Arizona, Tucson, AZ 85721-0001, USA; [7]The Santa Fe Institute, 1399 Hyde Park Road, Santa Fe, NM 87501, USA

Author for correspondence:
Gregory P. Asner
Tel: +1 650 325 1521
Email: gpa@carnegiescience.edu

Received: *8 February 2016*
Accepted: *16 May 2016*

New Phytologist (2017) **214:** 973–988
doi: 10.1111/nph.14068

Key words: canopy chemistry, Carnegie Airborne Observatory, Peru, plant functional traits, trait distributions, trait scaling.

Summary

- Average responses of forest foliar traits to elevation are well understood, but far less is known about trait distributional responses to elevation at multiple ecological scales. This limits our understanding of the ecological scales at which trait variation occurs in response to environmental drivers and change.
- We analyzed and compared multiple canopy foliar trait distributions using field sampling and airborne imaging spectroscopy along an Andes-to-Amazon elevation gradient. Field-estimated traits were generated from three community-weighting methods, and remotely sensed estimates of traits were made at three scales defined by sampling grain size and ecological extent.
- Field and remote sensing approaches revealed increases in average leaf mass per unit area (LMA), water, nonstructural carbohydrates (NSCs) and polyphenols with increasing elevation. Foliar nutrients and photosynthetic pigments displayed little to no elevation trend. Sample weighting approaches had little impact on field-estimated trait responses to elevation. Plot representativeness of trait distributions at landscape scales decreased with increasing elevation. Remote sensing indicated elevation-dependent increases in trait variance and distributional skew.
- Multiscale invariance of LMA, leaf water and NSC mark these traits as candidates for tracking forest responses to changing climate. Trait-based ecological studies can be greatly enhanced with multiscale studies made possible by imaging spectroscopy.

Introduction

Multiple foliar chemical traits link plant canopies to ecosystem energy exchange, biogeochemical cycles, and multitrophic interactions. For example, leaf Chl, nitrogen (N) and phosphorus (P) play key roles in light capture and photosynthesis, and leaf N and P also modulate decomposition and nutrient cycling rates (Schlesinger, 1991). Photosynthesis drives the production of nonstructural carbohydrates (NSCs), which can be stored and converted to more complex carbon compounds (e.g. cellulose, lignin) supporting longer-lived tissues in wood and roots (Dietze *et al.*, 2014). Foliar defense is also supported via the production of polyphenols and other compounds derived from NSC. These structural and chemical defense compounds mediate leaf turnover, herbivory, decomposition and nutrient release in soils. An integrative metric of leaf construction cost is dry mass per unit leaf area (LMA) (Poorter *et al.*, 2009). Together, these and other foliar traits reflect the evolution of plant strategies and adaptation to environment (Westoby & Wright, 2006; Agrawal, 2007).

Although we have learned a great deal about the functional importance of foliar chemical traits, our knowledge weakens when it comes to the ecological scales at which trait variation occurs. The interactive role of biogeographic and evolutionary processes, combined with environmental filtering and change, generates a complex ecological mosaic that challenges past approaches to investigating controls on the distributions of traits in space and time. In this context, elevation gradients have long been used to explore plant trait responses to the environment, particularly temperature. Large increases in elevation can drive

See also the Commentary on this article by McDowell & Xu, **214**: 903–904.

major changes in community-averaged leaf traits (Körner *et al.*, 1988; Cordell *et al.*, 1998), yet we know far less about how elevation and other associated environmental filters relate to plant trait distributions at multiple spatial scales. This, in turn, limits our ability to model and predict spatial variation in ecosystem processes at any given point along an elevation gradient, or over the entire elevation range in question. Should we work with average traits, their variances, and/or their particular distributions? This question will continue to grow in importance as dynamic vegetation models increasingly call for plant trait data to improve predictions of biospheric response and feedbacks to climate change (Sakschewski *et al.*, 2015).

One of the largest, contiguously vegetated elevation gradients in the world is located at the interface of the tropical eastern Andes and the western lowland Amazon basin in Perú (Malhi *et al.*, 2010). Throughout this region, elevation, with associated changes in climate and soils, is clearly linked to plant compositional turnover (von Humboldt, 1850; Gentry, 1988). Average forest structure, biomass, productivity and carbon cycling also change with elevation in this region (Girardin *et al.*, 2013; Asner *et al.*, 2014a; Metcalfe *et al.*, 2014). These ecosystem-level responses to elevation suggest that plant functional traits, many of which underpin physiological adaptations to elevation factors such as temperature, may also change. This hypothesis was supported in a recent field-based, leaf-level study along the Andes–Amazon elevation gradient, which revealed systematic shifts in average foliar traits within communities (Asner *et al.*, 2014b). They found that average LMA and NSC concentrations increased with elevation, but that mean foliar N declined very weakly and foliar P showed no trend. Although this study and a global compilation of field-based elevation data on foliar traits (Asner & Martin, 2016) produced similar patterns, neither study provided an understanding of whether foliar trait distributions change within and among communities along tropical forest elevation gradients.

To develop robust distributions of plant traits, the measurements must resolve the contributions of many individual plants within and across diverse environmental gradients (e.g. elevation, climate, soils). Yet understanding how the mean, variance and higher-order moments of plant traits vary environmentally remains a major challenge. The most common way to estimate trait distributions is through field sample collections, which are labor-intensive, difficult to repeat and may not adequately capture distributions or mean values. Trait distributions derived from field collections can also be sensitive to sampling approach. Typical approaches include: simply assessing traits as unweighted means of the most common species in a plot; sample collections weighted by stem number abundance; and sample collections weighted by species basal area (BA). Each approach has its strengths and limitations (Cornelissen *et al.*, 2003), and yet the relationship between each approach remains poorly documented, particularly in forests. We might expect that all three field-sampling approaches would converge on similar results for monotypic stands or very highly diverse canopies, as the effects of stem number- or BA-weighting diminishes in these situations. It is less clear what happens when canopies fall between these two extremes. Moreover, the spatial scale dependence of plant trait distributions is unknown because spatially continuous measurements are not available from field-based approaches.

Remote sensing offers a way to conduct spatially explicit assessments of some canopy traits and their distributions. In particular, imaging spectroscopy now provides estimates of various foliar traits (Kokaly *et al.*, 2009; Ustin *et al.*, 2009), affording a way to derive trait distributions at landscape to regional scales. Asner *et al.* (2015a) developed tropical canopy foliar trait distributions in a small network of lowland Amazonian forest landscapes in southern Peru, revealing substantial effects of soil type and microtopography on the distributions of multiple traits. However, their work did not consider changes in elevation. Moreover, their work was carried out over thousands of hectares of forest at a spatial grain size (resolution) of 1 ha, thereby averaging over a large number of canopies per sample trait estimate. No study has considered the effects of grain size or spatial extent in determining trait distributions. This may be particularly important given that future orbital imaging spectrometer missions may provide trait data at grain sizes of *c.* 0.1–0.5 ha resolution (Stuffler *et al.*, 2009; Lee *et al.*, 2015). Current airborne and future spaceborne remote sensing may generate plant trait distributions over large spatial extents, but only at a resolution that is much more coarse than subcanopy leaf collections undertaken in the field. As a result, there is a growing need for evaluating the compatibility of remote sensing and field-based approaches for plant trait distribution studies. We might expect that stem number- or BA-weighting of field-based foliar trait estimates would be more closely linked to remotely sensed estimates of traits. To our knowledge, however, these possibilities have not been tested in any ecosystem.

Despite the cumulative information gained along the Andes–Amazon elevation gradient in past studies, little is known about canopy chemical trait distributions at multiple ecological scales, as defined by spatial extent and measurement grain size (or resolution), because spatially contiguous and extensive data have only recently become available. Furthermore, no field or remote sensing studies have assessed changes in trait distributions with elevation in humid tropical forests. We estimated canopy foliar trait distributions and elevational trends using three plot-based sampling approaches, and compared the results with spatially continuous estimates of traits derived from airborne imaging spectroscopy at plot and landscape levels. We asked the following questions. How do field-based estimates of foliar traits vary within 1.0 ha plots along this tropical elevation gradient, and do different field sample weighting approaches result in different trait distribution estimates? How do estimated trait distributions derived from field sampling compare to those generated through airborne imaging spectroscopy? How do sampling grain size and ecological extent affect canopy foliar trait distribution patterns along the elevation gradient?

Materials and Methods

Elevation gradient

Our study was conducted based on an environmental stratification by elevation and soils of nine landscapes of *c.* 1000 ha each,

each containing a permanent 1.0 ha plot stretching from the lowland Peruvian Amazon to the treeline in the eastern Andes (Table 1; Fig. 1). The plots and their surrounding landscapes ranged in elevation from 215 to 3557 m above sea level (asl). Two lowland Amazonian landscapes are located in the Tambopata River basin, one of which (TAM-06; 215 m asl) is found on floodplain alluvium soils (Cambisols) and the other (TAM-05; 223 m asl) on elevated clay *terra firme* soils (Alisols). Another landscape (PAN-02) is situated on a foreland front range of the Andes (Plinthosols; 595 m asl) at the transition from submontane to lowland forest ecosystems. The remaining submontane and montane landscapes occupy the Kosñipata Valley in the province of Paucartambo, Region of Cusco (1527–3537 m asl; Cambisols and Umbrisols).

The forest plots are maintained by the Andes Biodiversity Ecosystems Research Group (ABERG, http://www.andesconservation.org) and the Amazon Forest Inventory Network (RAINFOR; http://www.rainfor.org), and are part of the ForestPlots (https://www.forestplots.net/) and Global Ecosystems Monitoring Network (GEM; http://gem.tropicalforests.ox.ac.uk/projects/aberg) networks. The plots are positioned in areas of relatively homogeneous soil substrate and stand structure, which have minimal evidence of human disturbance (Girardin *et al.*, 2013). From February 2013 to January 2014, mean annual air temperature varied from 9 to 24.4°C and precipitation ranged from 1560 to 5302 mm yr^{-1} across all plots along the gradient (Table 1).

Field sampling

From April to November 2013, we collected canopy samples in each of the nine 1.0 ha field plots. Based on the most recently available census and diameter data for each plot, a sampling protocol was adopted wherein species were sampled that maximally contributed to plot BA (a proxy for plot biomass or crown area). We aimed to sample the minimum number of species that contributed to 80% of BA, although in the diverse lowland forest plots we were only able to sample species comprising 60–70% of plot BA (Table 1). For each selected species, three to five individual trees were chosen for sampling (five trees in submontane and montane plots; three trees in lowland plots). If three trees were not available in the plot, we sampled additional individuals of the same species from an area immediately surrounding the plot.

Leaf collections were conducted using tree-climbing techniques. For each tree, fully sunlit branches at the top of the canopy were selected and cut, sealed in large polyethylene bags to maintain moisture, stored on ice in coolers, and transported to a local site for processing within 3 h, and usually < 30 min. A subset of fully expanded leaves was randomly selected from the branches for scanning to determine leaf area, and weighing to record FW and DW for determination of leaf water concentration. Additional leaves were selected for oven-drying at 70°C and another for acquisition of fresh leaf disks to be immediately frozen to −80°C in liquid N. Both subsets were maintained in their stabilized state for subsequent chemical analyses in the Carnegie Spectranomics Library (Stanford, CA, USA). Values of fresh leaf area were divided by DW to determine LMA.

Table 1 Environmental characteristics and plant sampling information for the 1.0 ha study plots along an Andean–Amazon elevation gradient

	Tambopata 6	Tambopata 5	Pantiacolla 2	San Pedro 2	San Pedro 1	Trocha Union 4	Esperanza	Wayqecha	Acjanaco
Site code	TAM-06	TAM-05	PAN-02	SPD-02	SPD-01	TRU-04	ESP-01	WAY-01	ACJ-01
Latitude	−12.8385	−12.8309	−12.6495	−13.0491	−13.0475	−13.1055	−13.1751	−13.1908	−13.1468
Longitude	−69.2960	−69.2705	−71.2626	−71.5365	−71.5423	−71.5893	−71.5948	−71.5874	−71.6323
Elevation (m)	215	223	595	1494	1713	2719	2868	3045	3537
Slope (°)	2.2	4.5	11.5	27.1	30.5	21.2	27.3	30.3	36.3
Aspect (°)	169	186	138	125	117	118	302	112	104
Solar radiation (GJ m^{-2} yr^{-1})	4.80	4.80	3.82	4.08	4.36	3.49	–	3.51	4.60
Mean annual temperature (°C)	24.4	24.4	23.5	18.8	17.4	13.5	13.1	11.8	9.0
Precipitation (mm yr^{-1})	1900	1900	2366	5302	5302	2318	1560	1560	1980
Soil moisture (%)	35.5	21.8	–	37.3	37.6	37.3	24.3	23.1	–
Mean canopy height (m)*	28.2	27.5	24.4	22.8	14.0	15.7	16.9	14.3	12.5
Soil type	Alisol	Cambisol	Plintosol	Cambisol	Cambisol	Umbrisol	Umbrisol	Umbrisol	Cambisol
Number of plant families	13	17	10	20	23	12	10	9	8
Number of plant genera	20	23	11	25	26	13	10	10	8
Number of plant species	20	27	14	26	29	18	14	14	11
Number of plant individuals	60	75	39	80	75	81	62	60	46

*Asner *et al.* (2014a).
Solar radiation measurements at Esparanza, and soil moisture data for the two sites added during this campaign (Pantiacolla and Acjanaco) are not yet available ('–').

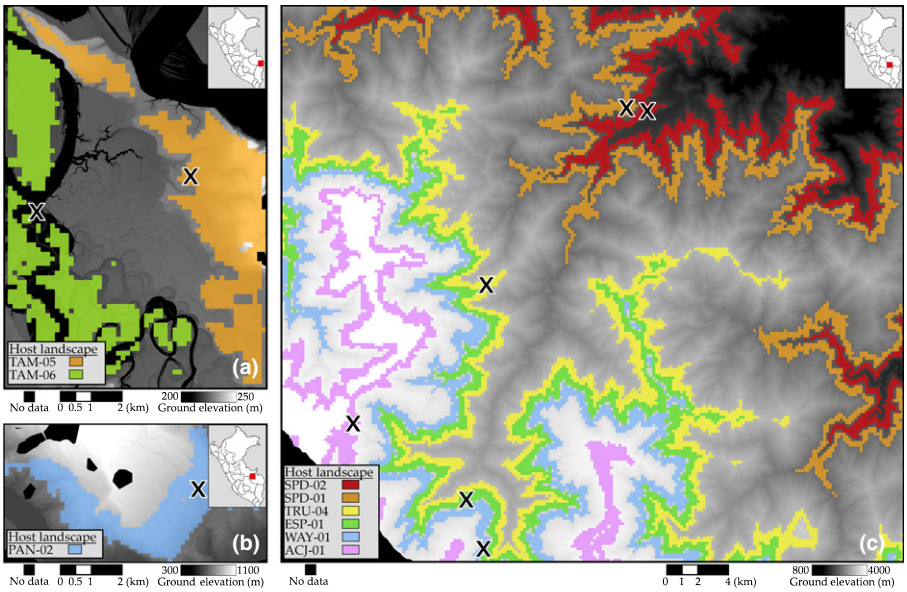

Fig. 1 Geographic distribution of nine forest elevation classes containing 1.0 ha study plots marked with 'X', which are also shown in Fig. 2. (a) Lowland landscapes hosting TAM-05 and TAM-06 plots on *terra firme* (terrace) and floodplain substrates, respectively. (b) Submontane PAN-02 landscape. (c) Submontane to montane landscapes SPD-01, SPD-02, TRU-04, ESP-01, WAY-01 and ACJ-01. Inset maps of Peru indicate the approximate location of each landscape at the red square. Descriptions for each field site are provided in Table 2.

Laboratory assays

Chemical analysis protocols and instrument information are downloadable from the Carnegie Spectranomics Project website (http://spectranomics.ciw.edu) and are summarized here. Dried foliage was ground in a 20 mesh Wiley mill. P concentration was determined in 0.4 g dry leaf tissue by inductively coupled plasma optical emission spectroscopy (Therma Jarrel-Ash, Waltham, MA, USA) after microwave digestion in 10 ml (70% concentration) nitric acid solution (CEM MARSXpress, Matthews, NC, USA). One blank and two reference standards (Peach NIST SRM 1547 and internal lemon leaf) were digested and measured with each set of 40 foliar samples to track the reproducibility and accuracy of the method.

Carbon fractions including NSC and lignin were determined in 0.5 g dry ground leaf tissue through using sequential digestion of increasing acidity in a fiber analyzer (Ankom Technology, Macedon, NY, USA). Carbon fractions are presented on an ash-free dry mass basis following ignition of the remaining sample at 500°C for 5.5 h. We note that our NSC determinations include sugars, starch and soluble components of pectin, and thus may be at overall higher concentration than more narrow definitions of total NSC (Quentin *et al.*, 2015). An internal lemon leaf standard was used as a reference with each run to ensure consistency across runs. This standard is available upon request for use in converting our estimates to those found elsewhere in the literature. A subset of the ground material was further processed to a fine powder for determination of total N concentration by combustion-reduction elemental analysis (Costec Analytical Technologies Inc., Valencia, CA, USA).

Frozen leaf disks were used for the total Chl and phenolic determinations. For phenols, disks were ground in 95% methanol using a high-throughput tissue homogenizer. A portion of the solution was further diluted and incubated on an orbital shaker at room temperature (15–18°C) in the dark for 48 h to ensure proper phenol extraction. The total phenolic concentration in solution was determined colorimetrically using the Folin-Ciocalteau method. Phenol concentrations were measured in gallic acid equivalents relative to an eight-point Gallic acid standard curve. Total Chl concentration was quantified using two frozen leaf disks (1.54 cm^2). These disks were rapidly ground in 1.5 ml centrifuge tubes containing 0.75 ml 100% acetone on a high-throughput tissue homogenizer (Troemner, Thorofare, NJ, USA) with a small amount of $MgCO_3$ to prevent acidification. Following dilution and centrifugation for 3 min at 2000 ***g***, the absorbance of the supernatant was measured using a dual-beam scanning UV-VIS spectrometer (Lambda 25, Perkin Elmer, Beaconsfield, UK).

Comparing field-based estimates of foliar traits

In the previous foliar trait study on this elevation gradient, Asner *et al.* (2014b) found that interspecific variation far exceeded intraspecific variation for most traits, and strong phylogenetic partitioning of traits remained evident within communities, despite community-scale shifts in many traits. This indicated that trait variation along the elevation gradient is the result of differential and nonrandom species sorting, rather than plasticity. This is important here because it suggests that capturing elevation trends in canopy foliar traits requires sampling strategies that integrate a large number of taxa per site. The Asner *et al.* (2014b) sample collections were based on a phylogenetic approach with replication of the top 15% most common species at each site. In the present paper, we test three more common sampling schemes, each of which is based on collection of the most common species in each plot: unweighted – plot values and distributions calculated simply from all individual samples; species stem number weighting by the number of individuals; and BA weighting by the sum of the squared tree diameters at breast height. We used ordinary least-squares regression to assess relationships among leaf traits, elevation and each of the three sampling approaches. We assessed the adequacy of sampling method by quantifying the

interactions between elevation and sampling approach for each trait. If there is no interaction between elevation and sampling approach, then the regression slopes for each method will be parallel. The trait data were a subset of the full census data, so the species mean values were assigned to their corresponding taxa in the census, thus permitting the stem number and BA values to be used. Species stem number- or BA-weighted mean values for each trait in each plot were calculated as:

$$\bar{x}_w = \frac{\sum_{i=1}^{N} W_i \cdot x_i}{\sum_{i=1}^{N} x_i}$$

where x_w is the weighted mean trait value for the plot, x_i is the mean trait values for species i at a given plot and w_i is the weight for the i^{th} species. The corresponding weighted standard deviation (SD) for each trait was calculated as:

$$\sigma_w = \sqrt{\frac{\sum_{i=1}^{N} w_i \cdot (x_i - \bar{x}_w)^2}{\frac{(N'-1)\sum_{i=1}^{N} w_i}{N'}}}$$

where σ_w is the weighted SD for the plot and N' is the number of nonzero weights.

Remote sensing

Airborne remote sensing data were acquired in August 2013, coinciding with the field campaign, using the Carnegie Airborne Observatory-2 (Asner *et al.*, 2012), which included a high-fidelity visible-to-shortwave infrared (VSWIR) imaging spectrometer and a dual-laser waveform LiDAR. We collected the data over each study landscape from an altitude of 2000 m above ground level (agl) at an average flight speed of 55–60 m s^{-1}. The VSWIR spectrometer measures spectral radiance in 427 channels spanning the 380–2510 nm wavelength range in 5 nm increments (full-width at half-maximum). The VSWIR has a 34° field-of-view and an instantaneous field-of-view of 1 mrad. At 2000 m agl, the VSWIR data collection provided 2.0 m ground sampling distance, or pixel size, throughout each study landscape. The LiDAR has a beam divergence set to 0.5 mrad and was operated at 200 kHz with 17° scan half-angle from nadir, providing swath coverage similar to the VSWIR spectrometer. The LiDAR point density was two laser shots m^{-2}, or eight shots per VSWIR pixel. The LiDAR data were combined with an embedded high-resolution global positioning system-inertial measurement unit (GPS-IMU) data to produce a cloud of georeferenced point data. Digital terrain models, digital surface models (DSMs) and digital canopy models (DCMs) were calculated using the method described in Asner *et al.* (2012).

The VSWIR data were radiometrically corrected from raw DN values to radiance (W m^{-2} sr^{-1} nm^{-1}) using a flat-field correction, radiometric calibration coefficients and spectral calibration data collected in the laboratory. The standardized GPS pulse-per-second measurement was used to precisely colocate VSWIR spectral imagery to the LiDAR data using the technique detailed by Asner *et al.* (2012). The VSWIR radiance data were atmospherically corrected using the ACORN-5 model (Imspec LLC, Glendale, CA, USA), along with a method for minimizing variations in atmospheric aerosol effects (Colgan *et al.*, 2012). The VSWIR imagery was then orthorectified to the LiDAR DSM. The CAO VSWIR images for the nine 1.0 ha plots and immediate *c.* 8 ha surroundings are shown in Fig. 2, which are color-infrared composites of spectral bands centered at 800, 680 and 550 nm. The data values in these images are histogram-matched to the full range of values across all images to allow for visual comparison of canopy greenness and forest cover.

Conversion of the VSWIR spectra to estimates of canopy foliar traits followed the method detailed by Asner *et al.* (2015b). First, the coaligned VSWIR and LiDAR data were processed together to develop a suitability map for leaf trait estimation. This suitability map was based on the following filtering criteria: normalized difference vegetation index (NDVI) ≥ 0.8; vegetation height ≥ 2.0 m; and minimal intra- or intercanopy shade in the VSWIR pixel. Through a survey of >7 million ha of VSWIR imagery over Andean and Amazonian forests, we have found that a minimum NDVI threshold of 0.8 is highly conservative, allowing most tropical canopy foliage into the trait analysis, while excluding areas of unfoliated canopy. The 2.0 m minimum height requirement removes bare ground and short nonforest vegetation such as exposed grass cover. The shade mask is derived from a ray tracing model that precisely identifies canopy location in unshaded and unobstructed view of the VSWIR spectrometer (Asner *et al.*, 2007). This LiDAR-based shade mask removes VSWIR pixels that are fully or partially shaded by adjacent foliage, branches or crowns. Together, these filters provided a pixel-by-pixel suitability map from which spectral reflectances can be selected for analysis. This filtering technique has the advantage of reducing the total canopy analysis area to a value analogous to the 'sunlit canopy foliage' criterion used in field collections of forest canopy foliage.

Following the preparation of the filtered VSWIR reflectance spectra, we convolved them to 10 nm bandwidth and applied a brightness-normalization adjustment (Feilhauer *et al.*, 2010). Brightness normalization utilizes 'spectral angle' to mitigate differences in brightness that may arise from internal canopy shade, which is proportional to LAI (Myneni *et al.*, 1989; Kruse *et al.*, 1993). This reduces the contribution of varying LAI to chemometric determinations of foliar traits from remotely sensed data (Feilhauer *et al.*, 2010). The resulting spectra were trimmed at the ends (<410 nm, >2450 nm) of the measured wavelength range, as well as in regions dominated by atmospheric water vapor (1350–1480, 1780–2032 nm). We used partial least-squares regression (PLSR; Haaland & Thomas, 1988) to quantitatively convert the airborne VSWIR spectroscopy to estimates of foliar traits using the method and equations provided by Asner *et al.* (2015b). The PLSR approach is beneficial because it utilizes the continuous spectrum as a single measurement rather than in a band-by-band type of analysis (Martens, 2001; Boulesteix & Strimmer, 2006). To avoid statistical over-fitting, the number of orthogonal spectral dimensions or vectors used in the PLSR analysis was estimated by minimizing the prediction residual error

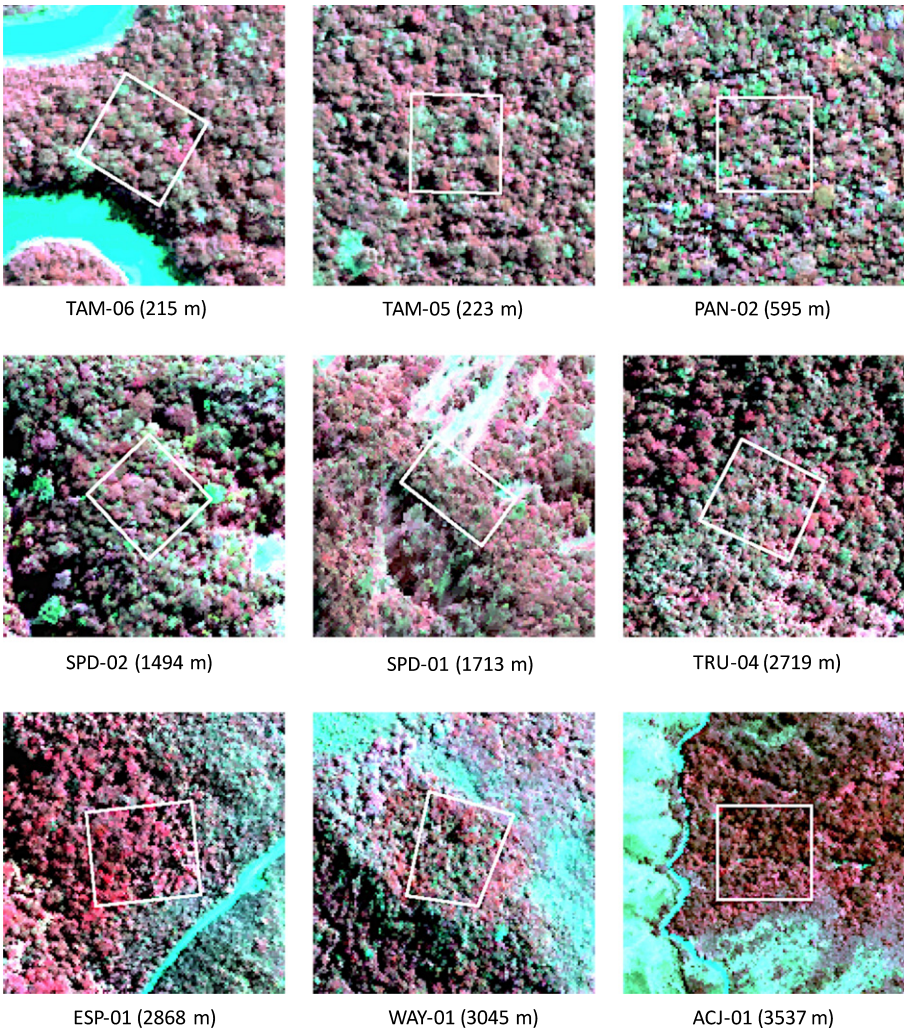

Fig. 2 Color-infrared composite images derived from Carnegie Airborne Observatory (CAO) visible-to-shortwave infrared (VSWIR) imaging spectroscopy of the 1.0 ha field plots arrayed along the Andes–Amazon elevation gradient (see Fig. 1 for plot locations). Red, foliated vegetation; blue, rivers, roads, and/or senescent vegetation.

sum of squares statistic (Chen *et al.*, 2004). This method has been tested and validated in the Peruvian Amazon at a series of sites not included in the present study, but which span a wide range of forest ecological conditions in the western Amazon and Andean region (Asner *et al.*, 2015b).

After obtaining estimates of foliar traits at the nominal 2 m VSWIR sampling resolution, we averaged the data to 0.01 ha (10 m × 10 m) and 1.0 ha (100 m × 100 m) grain sizes for analysis. We selected the 0.01–1.0 ha extremes to bracket the range of measurement resolutions that will become available from Earth orbit. Additionally, the 0.01 ha grain size provided a means to smooth any spurious measurements that were not removed during the filtered described earlier, and it is about the lower limit for 'pairing' field-based sampling grain size to remotely sensed sampling. We used the 0.01 ha data within the 1.0 ha field plots to generate remotely sensed trait distributions for each plot. We also randomly sampled 400 points at the 0.01 and 1.0 ha resolution within each 1000 ha landscape. The 1.0 ha grain size is useful because it matches the intended resolution of field sampling in 1.0 ha plots, and because it probably represents the coarsest resolution for future spaceborne imaging spectrometer missions. Note that the highest elevation ACJ-01 landscape, which is on the forest–grassland transition at treeline, is very small overall (77 ha), so we randomly sampled 40 forested 0.01 and 1.0 ha points surrounding the field plot. Finally, the Moran's I statistic was used to assess spatial autocorrelation of the canopy chemical. Results indicated Moran's I values < 0.21 at the plot level and 0.17 at the landscape level, thereby indicating low spatial autocorrelation of the image-based data.

Results

Field-based trait estimates

We found strong linear increases in community-mean LMA, NSC and leaf water concentration with increasing elevation, independent of sample weighting approach (Fig. 3; Table 2; Supporting Information Table S1). Foliar N displayed a modest decrease (regression slopes = −15% to −20%) with increasing elevation. Neither foliar Chl nor P displayed a significant trend with elevation using any sample weighting approach. Defense-related traits showed weak to variable signs of change with elevation. Lignin declined only for the unweighted field estimates. Total phenols substantially increased with elevation, but then

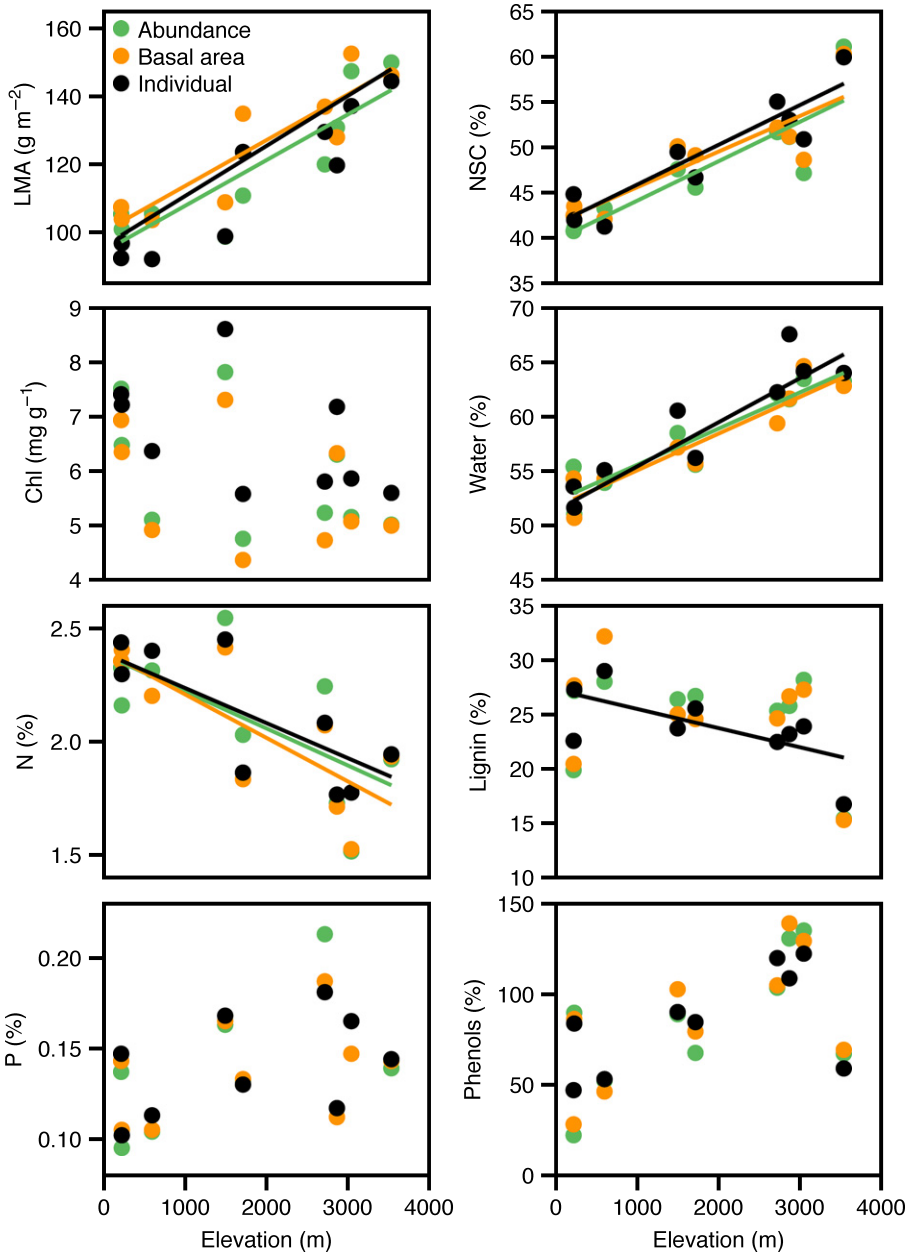

Fig. 3 A comparison of field-based estimates of mean canopy foliar trait values as a function of elevation. Field data are presented as unweighted means among all individuals (black), stem number abundance-weighted means (green), and basal area-weighted means (orange). LMA, leaf mass per unit area; N, nitrogen; P, phosphorus; NSC, nonstructural carbohydrates. Detailed statistical information for each site is provided in Supporting Information Table S1.

declined sharply at the highest elevation site (ACJ-01; Fig. 3). This resulted in nonsignificant regressions against elevation (Table 2). Trait variances (SDs) showed little to no trend with increasing elevation (Table S1), with the exception of LMA, which underwent an overall increase in variation with increasing elevation.

The method for weighting the field data – unweighted, stem number-weighted or BA-weighted – played very little role in estimating the community-mean elevation trends in trait values (Table S2). Moreover, for almost every foliar trait tested, differences in sample treatment weighting approach had no effect on estimates of variance, skewness or kurtosis (Table S2). This resulted in very similar regression equations, R^2-values, and root-mean-squared error relating elevation to each field-sampled foliar trait (Table 2). Given the similarity in foliar distributions and elevation trends among the field-based weighting approaches, we carried forward only the unweighted field-based results to compare against the remotely sensed traits.

Trait patterns and distributions

Visually there was no obvious elevation-based pattern in canopy reflectance as viewed simply in the color-infrared images (Fig. 2) or in natural color composite images (not shown). However, conversion of the VSWIR imaging spectroscopy data to canopy chemical maps did reveal elevational trends, such as shown in Fig. 4. In this example set of data outputs, the chemical images visually indicate that LMA (red) and NSC (green) increase with elevation, whereas Chl (blue) shows no clear trend. Despite these basic trends, the plots and surrounding landscapes remain highly

Table 2 Relationships between elevation and site-level mean canopy foliar traits along an Andes–Amazon elevation gradient in Peru, using six different sampling approaches: field-based leaf collections in 1.0 ha plots without weighting and with abundance- and basal area-based weighting; remote sensing (RS) at 0.01 ha resolution within 1.0 ha plots; and remote sensing at 0.01 and 1.0 ha resolution in up to 1000 ha landscapes centered on each field plot

	Field		Remote sensing	
Trait	R^2 (RMSE)	Equation	R^2 (RMSE)	Equation
	Unweighted		*RS (0.01 ha) in 1.0 ha plots*	
LMA	0.86 (7.64)	$13.99x + 96.76$	0.94 (5.86)	$17.05x + 99.09$
Chl	ns	ns	0.88 (0.32)	$-0.64x + 6.10$
N	0.56 (0.18)	$-0.15x + 2.38$	ns	ns
P	ns	ns	ns	ns
NSC	0.86 (2.23)	$4.03x + 41.55$	0.87 (5.24)	$10.06x + 35.19$
Water	0.84 (2.41)	$4.03x + 51.41$	0.61 (2.39)	$2.17x + 52.84$
Lignin	0.47 (2.73)	$-1.88x + 27.55$	ns	ns
Phenols	ns	ns	ns	ns
	Abundance weighting		*RS (0.01 ha) in 1000 ha landscapes*	
LMA	0.80 (9.78)	$14.31x + 93.37$	0.87 (5.14)	$9.67 + 102.65$
Chl	ns	ns	0.73 (0.38)	$-0.46 + 6.98$
N	0.45 (0.27)	$-0.18x + 2.40$	ns	ns
P	ns	ns	ns	ns
NSC	0.79 (3.04)	$4.26x + 39.97$	0.81 (4.27)	$6.51 + 43.10$
Water	0.87 (1.71)	$3.26x + 52.39$	0.74 (2.05)	$2.54 + 53.30$
Lignin	ns	ns	ns	ns
Phenols	ns	ns	0.88 (3.61)	$7.22 + 101.12$
	Basal area weighting		*RS (1.0 ha) in 1000 ha landscapes*	
LMA	0.78 (10.04)	$14.01x + 99.54$	0.91 (4.95)	$11.60 + 100.26$
Chl	ns	ns	0.66 (0.33)	$-0.34 + 6.62$
N	0.61 (0.22)	$-0.20x + 2.42$	ns	ns
P	ns	ns	ns	ns
NSC	0.74 (3.12)	$3.84x + 42.03$	0.92 (3.73)	$9.25 + 40.78$
Water	0.87 (1.76)	$3.31x + 51.84$	0.69 (2.29)	$2.48 + 54.08$
Lignin	ns	ns	ns	ns
Phenols	ns	ns	0.63 (6.58)	$6.29 + 105.68$

Regression R^2 is shown, with root mean squared error (RMSE) in parentheses. The equations are reported relative to elevation (x) in km.
LMA, leaf mass per unit area; N, nitrogen; P, phosphorus; NSC, nonstructural carbohydrates; ns, not significant.

variable, which highlights the challenge of integrating sampling approach, grain size and extent to best estimate trait distributions.

The distributions of remotely sensed canopy traits varied with increasing elevation and sampling approach (Fig. 5), but several consistent patterns did emerge. For LMA, N, NSC, lignin and phenols, the variance in the distributions generally increased with increasing elevation (Table S3). This occurred for all remote sensing sampling grain sizes and extents, and it was independent of whether there was an elevational trend in the plot- or landscape-mean trait values. Importantly, the remotely sensed trait distributions within the field plots were not always representative of the remotely sensed distributions at landscape scales. Plot-scale representativeness of landscapes generally decreased with increasing elevation. At the landscape level, sampling grain size (0.01 vs 1.0 ha) had a relatively minor effect on trait distributions and their statistical moments (red and green lines in Fig. 5, and statistics in Table S3). One exception was NSC at upper submontane elevations. We also observed increasing left skew (left tail increasing) in the distributions with increasing elevation, particularly for Chl, N and lignin, and right skew in NSC distributions with increasing elevation (Fig. 5). This was also indicated in the statistical moment information provided in Table S3.

Field-based trait distributions were poorly related to the remotely sensed distributions along the elevation gradient, and this mismatch generally worsened with increasing elevation (Fig. 5). Within the 1.0 ha field plots, field sampling (dark blue dashed lines) and remote sensing (cyan dashed lines) rarely agreed. Understandably, plot-based field samples were more widely distributed than were the 0.1 ha resolution sampling of the airborne imaging spectrometer measurements. Plot-level remote sensing also produced smoother distributions that were closer to Gaussian in shape than was observed in the field sample-based distributions. As a result, elevation trends in both the means and distributions were more clearly depicted in the plot-scale remote sensing estimates of most traits.

Elevation and scale dependence of trait distributions

We further compared elevational trends in leaf trait distributions derived from field sampling within plots (unweighted samples only) to the 0.01 ha remotely sensed estimates within plots, as well as the 0.01 and 1.0 ha remotely sensed estimates at the landscape level (Fig. 6). With few exceptions, the differing scales of trait estimation showed similar elevation trends. For example, field and remotely sensed approaches indicated similar elevation

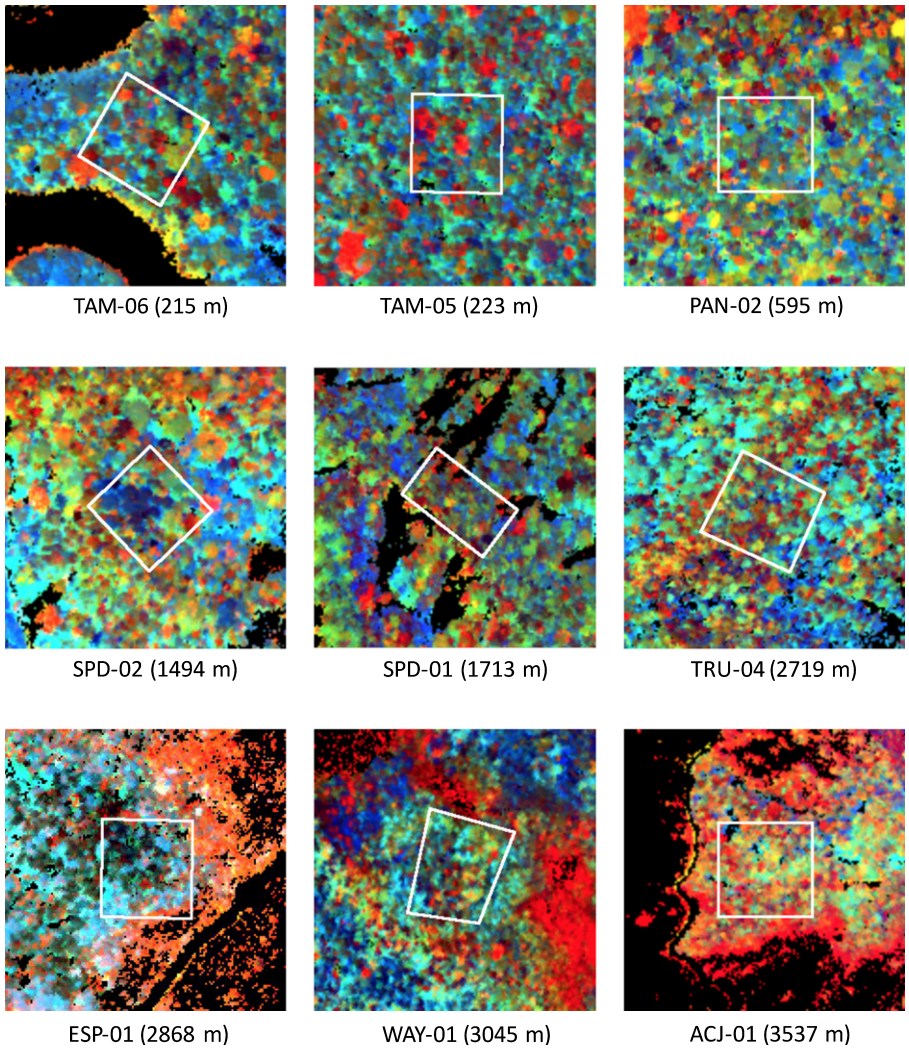

Fig. 4 Example imaging spectrometer composites showing differences in canopy leaf mass per area (LMA) in red, nonstructural carbohydrate (NSC) concentrations in green, and CHl*a* + *b* concentrations in blue, within and around the 1.0 ha study plots along the Andean–Amazon elevation gradient. See Fig. 1 for field site locations, and Fig. 2 for color-infrared composites of the source imagery.

trends for mean LMA and leaf water content (Table 2). NSC, which increased with elevation in the field samples, also did so in the remotely sensed data (Fig. 6e), but the rate of NSC change was greater using imaging spectroscopy (Table 2). This was also observed in the elevational trends among trait distributions (Fig. 5).

Foliar Chl showed no clear trend with elevation in the field samples (Fig. 6b; Table 2), but the higher sampling rate from remote sensing revealed statistically significant decreases in Chl with increasing elevation. Foliar N showed variable responses to elevation and sampling approach (Fig. 6c). Foliar N decreased with increasing elevation in the field sample-based estimates, but did not do so in the imaging spectrometer results at either plot or landscape scales. This was clearly evident in the trait distributions, which developed left skew with increasing elevation in both field and remotely sensed samples (Fig. 5). However, the skew was more pronounced in the field samples (Table S3). Foliar P showed no mean elevation trend using any approach at any ecological scale (Fig. 6d), although P did show slight left skew at the highest elevations (> 2500 m asl; Fig. 5).

Defense-related traits also displayed only minor elevational trend (Fig. 6g,h). Lignin decreased very slightly in the unweighted field samples, but did not significantly decrease in the remotely sensed data (Table 2). We note again that lignin did not decrease in the field samples when community means were calculated using either BA or stem number weighting (Fig. 2). Phenols showed only a slight increase with elevation in the field-based approaches (with the exception of a sharp decline at the highest elevation site; Fig. 2), which generally agreed with the remotely sensed sampling within the plots. However, phenols did increase in concentration with elevation in the remote sensing sampling at the landscape level (Fig. 6h), suggesting that the field plots are not representative of their host landscapes.

We assessed the relative importance of elevation and the unweighted field-based and three remotely sensed sampling approaches on foliar trait distributions as expressed in mean, SD, skewness and kurtosis (Tables 3, S3). Elevation, and not sampling approach, was the dominant factor determining mean changes in LMA, Chl, NSC, water and phenols. By contrast, sampling approach was more important than elevation in determining foliar N trends. Distributional variance (SD) of LMA was approximately equally driven by sampling approach and elevation, whereas sampling approach dominated the SD of all other foliar traits (Table 3). For both means and SD of the trait

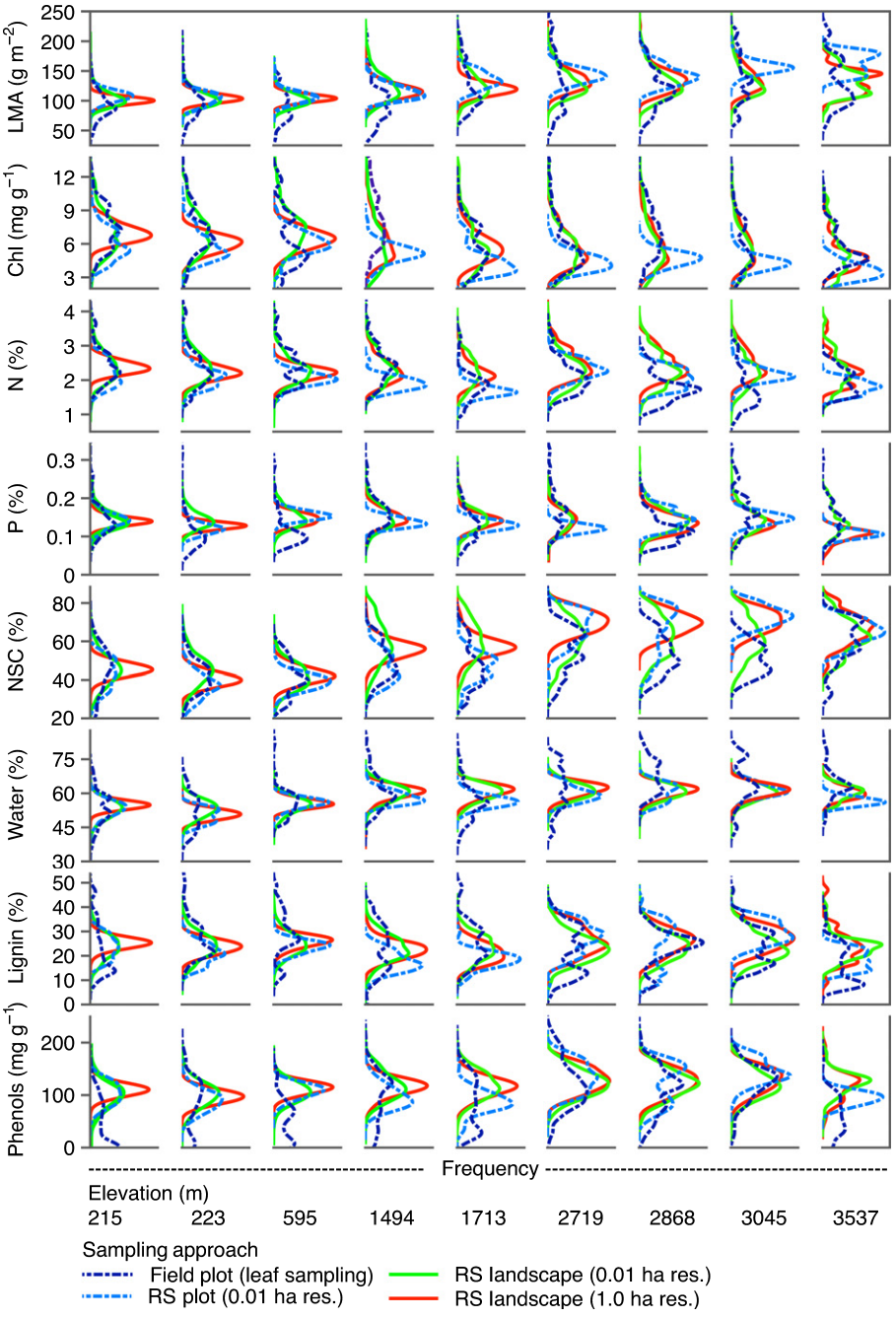

Fig. 5 Distributions of canopy foliar traits estimated at four ecological scales. Dark blue lines indicate distributions in traits from hand-collected leaf samples in 1.0 ha field plots (unweighted sample reporting from Fig. 2). Cyan lines are for remotely sensed (RS) traits at 0.01 ha spatial resolution in each 1.0 ha plot. Green and red lines are remotely sensed traits at 0.01 and 1.0 ha spatial resolution throughout each study landscape, respectively. LMA, leaf mass per unit area; N, nitrogen; P, phosphorus; NSC, nonstructural carbohydrates.

distributions, the interactions between sampling approach and elevation were generally weak but variable. The exception was foliar N, for which the interaction of sampling approach and elevation was about as important as the individual drivers in determining mean N values.

Higher-order moments of the trait distributions indicated variable effects of sampling approach (field or remote sensing) and elevation on the shape of the distributions (Table 3). Sampling approach had a strong effect on the skew and kurtosis of the LMA distributions. Moreover, the skew and kurtosis of foliar P distributions were sensitive to sampling approach, elevation, and their interaction. Other traits were more variably affected by either sampling approach or elevation, as seen in Fig. 5.

Discussion

Along this Andes–Amazon elevation gradient, multiple foliar traits shift their community-mean values, while others do not, and foliar trait distributions change substantially from lowland to montane tropical environments. Moreover, sampling approach, whether from field collections or remote sensing, as well as sampling grain size and extent have an important effect on the derived trait distributions. As a result, interpretations of plot-scale patterns, plot representativeness, and landscape-level shifts in canopy traits are partially dependent upon sampling approach.

Across our study gradient, field sampling revealed monotonic increases in LMA, with increasing variance but relatively constant

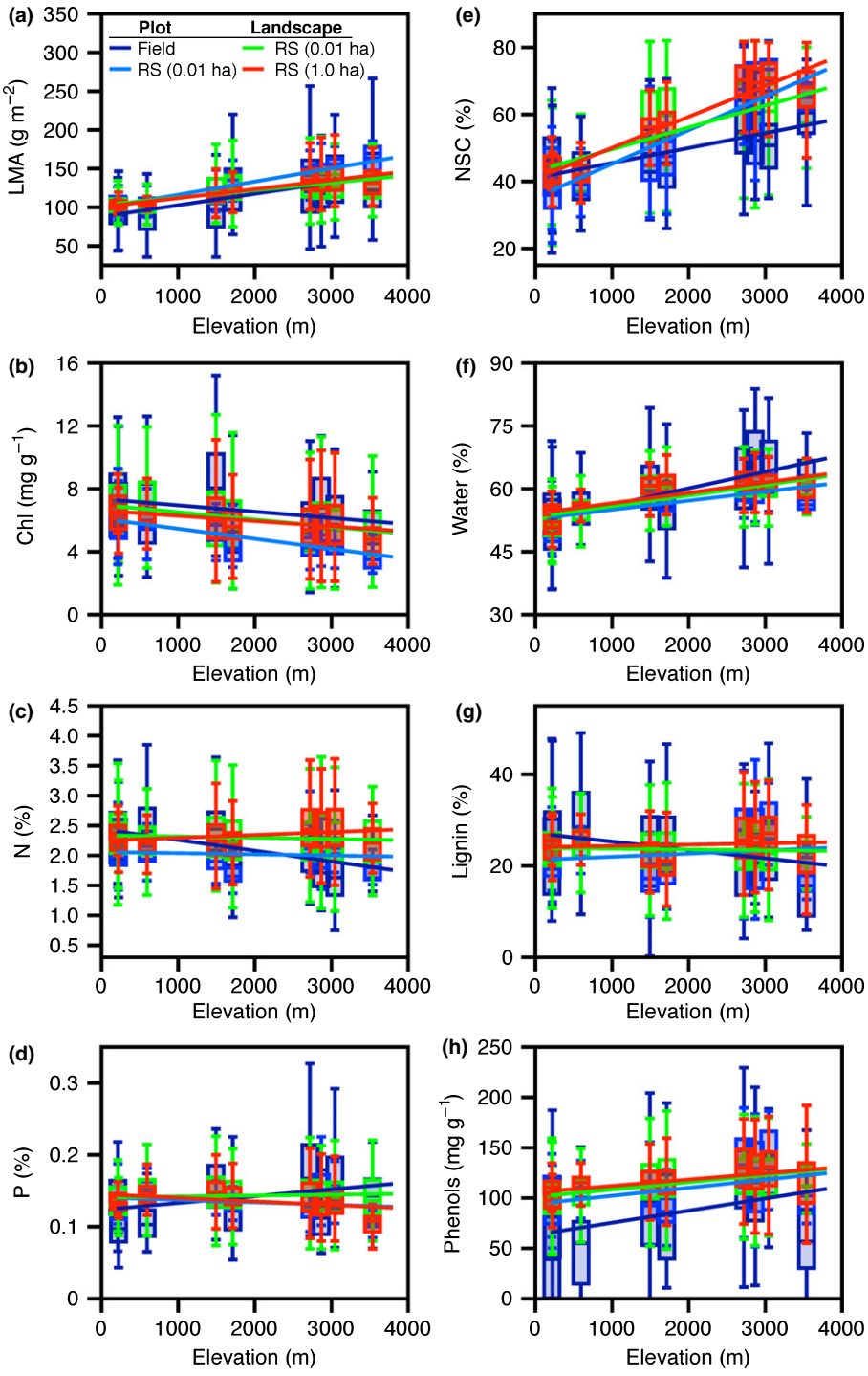

Fig. 6 Elevation dependence of canopy foliar traits estimated at four ecological scales: dark blue lines and boxes indicate trends in foliar traits collected by hand in the 1.0 ha field plots (unweighted sample reporting from Fig. 2); cyan lines and boxes are for remotely sensed traits at 0.01 ha spatial resolution in each 1.0 ha plot; green and red lines and boxes are remotely sensed traits at 0.01 and 1.0 ha spatial resolution throughout each study landscape, respectively. Error bars indicate ± 1SD about the mean value per site. LMA, leaf mass per unit area; N, nitrogen; P, phosphorus; NSC, nonstructural carbohydrates. Regression results are shown in Table 2.

distributional shape (skewness, kurtosis) within communities. Increases in mean LMA have been observed in elevation studies of both tropical and temperate vegetation (Körner *et al.*, 1986; Roderick *et al.*, 2000; Cornwell & Ackerly, 2009; Sides *et al.*, 2014). Higher LMA is associated with plant resource conservation strategies under increasingly adverse growing conditions. Although studies indicate that LMA and leaf water content are often anti-correlated (Roderick *et al.*, 2000), our results indicate that both increase with elevation. This may be because of a parallel increase in thickness of the foliage, allowing for more water content, with increasing elevation. The underlying drivers of changing LMA include a diverse array of climate and soil fertility factors (Poorter *et al.*, 2009). Temperature and radiation, and perhaps humidity, are among the most important on tropical elevation gradients, as observed by Cordell *et al.* (1998). Across our gradient, precipitation undergoes a mid-elevation peak but no overall trend, whereas temperature clearly declines with elevation (Table 1). Increasing community-mean LMA thus suggests

Table 3 Multiple linear regression model *F*-statistics relating canopy foliar traits along an Andes–Amazon elevation gradient in Peru, using four sampling approaches (SA): unweighted field-based leaf collections in 1.0 ha plots; remote sensing at 0.01 ha resolution within 1.0 ha plots; and remote sensing at 0.01 and 1.0 ha resolution in up to 1000 ha landscapes centered on each field plot

Trait	SA	Elevation	SA × elevation	SA	Elevation	SA × elevation
	Mean			Standard deviation		
LMA	9.9	250.0	3.8	55.9	65.2	5.2
Chl	14.0	34.2	ns	36.2	ns	6.5
N	9.1	4.3	5.5	44.0	ns	16.2
P	ns	ns	ns	32.5	6.4	ns
NSC	6.8	180.5	5.2	16.1	7.5	ns
Water	ns	79.5	ns	84.6	ns	ns
Lignin	ns	ns	ns	28.4	7.5	5.4
Phenols	7.1	13.9	ns	45.9	4.5	5.4
	Skewness			*Kurtosis*		
LMA	11.2	ns	ns	5.0	ns	ns
Chl	ns	ns	ns	ns	ns	ns
N	3.7	ns	5.6	ns	ns	ns
P	19.3	4.9	6.0	14.8	17.1	8.7
NSC	ns	ns	6.0	ns	ns	ns
Water	6.0	ns	ns	ns	ns	ns
Lignin	ns	ns	3.2	ns	ns	ns
Phenols	ns	ns	ns	ns	6.6	3.4

LMA, leaf mass per unit area; N, nitrogen; P, phosphorus; NSC, nonstructural carbohydrates; ns, not significant.

that temperature is a broad environmental filter of this trait. However, strong elevation-dependent increases in LMA variance (Fig. 5) also suggest that other microclimatic factors, such as radiation and humidity, may drive trait-based niche filling within communities at higher elevations.

Remotely sensed estimates of average changes in LMA and leaf water at all three spatial scales of analysis (0.01 ha within plots; 0.01 and 1.0 ha across landscapes) generally agree with the field-based sampling (Fig. 6). Similar results between the unweighted and weighted field samples, as well as with the fine-grain and coarse-grain remote sensing at contrasting spatial extents, suggest that LMA and leaf water shift with spatial consistency within and across ecosystems along the elevation gradient. Ecologically, this finding further suggests that community-scale distributions of LMA and leaf water shift in response to large-scale environmental drivers, while intracommunity variation is maintained by niche-based partitioning of resources (Cornwell & Ackerly, 2009).

Increases in LMA are often associated with decreases in mass-based foliar N concentration (Wright *et al.*, 2001) and reduced rates of nutrient supply via decomposition (Schuur & Matson, 2001; Nottingham *et al.*, 2012). In a fertilizer experiment along our gradient, Fisher *et al.* (2013) found some evidence for declining N availability with elevation, which would underpin our field-estimated declines in mean leaf N (Fig. 3). However, we had mixed results when comparing the elevation trends in foliar N using field and remote sensing approaches (Fig. 6). The uncertainty results from a combination of factors affecting the derived N distributions and the sensitivity of each sampling approach. First, field-based and remotely sensed N distributions showed increasing left skew with increasing elevation (Fig. 5; Table S3). This suggests similar overall trending among sampling approaches. However, the left skewing of the distributions was more pronounced in the field samples, relative to the remotely sensed samples, and this generated the differences in the mean trends between approaches. While the community-mean values shifted downward with elevation in the field samples, but not the remotely sensed samples, the community medians did shift downward using all sampling approaches. Second, a field study by Asner *et al.* (2014b) found a 13–18% decline in foliar N concentration with increasing elevation, a result based on thousands of canopies and species throughout the region. Our field data show a foliar N decline of 15–20% depending upon how the samples are weighted locally. However, the remote sensing method used here reports an absolute uncertainty of 0.3 ± 0.06 mg g^{-1} (Asner *et al.*, 2015b), which equates to similar variation (*c.* 15%) of the range observed in the field samples across our elevation gradient (Fig. 2). Site-by-site comparisons between field-based and remotely sensed estimates of foliar N show little to no statistical differences at lower elevations (< 1500 m), above which the field-based measurements decline as the remote sensing estimates remain more constant. It is therefore unsurprising that the field and remote sensing approaches do not agree on a mean elevation trend for this set of nine plots and their surrounding landscapes.

When foliar N is examined on an area basis, both field and remote sensing approaches indicate increasing area-based N with elevation, although the field estimates change at a lower rate (Fig. S1). Because there is no obvious pattern to solar radiation across the sites (Table 1), the trend of increasing area-based N with increasing elevation is probably a result of decreasing temperatures, which fall from 24 to 9°C. This pattern has been documented in other studies and may be associated with increasing mesophyll layer thickness (Körner *et al.*, 1986; Hikosaka *et al.*, 2002). This may also explain the higher water content in the leaves at higher elevations. An important next step is to map additional elevation gradients with the goal of clarifying these

and other subtle changes in foliar nutrient concentrations by integrating over larger areas. This could be particularly useful given the persisting paradigm that montane tropical forest productivity is N-limited, whereas lowland forests are P-limited (Townsend *et al.*, 2008). If foliar chemistry is reflective of nutrient limitation (Vitousek, 1982), our overall findings suggest no strong elevation trend in N or P limitation on this particular gradient.

We measured a 50–70% increase in foliar NSC concentration in canopies along the elevation gradient, with remote sensing producing the steeper elevation trend (Fig. 6). Within-community variation in foliar NSC also increased substantially at higher elevations. Asner *et al.* (2014b) suggested that increasing NSC concentrations with elevation could be related to increased waxiness or to reductions in the conversion of NSC to cellulose at higher elevations. Although leaf waxes do increase with elevation, they account for far less than 1% of leaf mass and are uncorrelated with NSC along our Andes–Amazon gradient (S. J. Feakins & T. Peters, unpublished). The possibility of an NSC-to-cellulose conversion bottleneck remains supported by an observed decrease in foliar Ca with elevation (Asner *et al.*, 2014b), because Ca plays a crucial role in the conversion of NSC to cell walls (Demarty *et al.*, 1984; Gilliham *et al.*, 2011). Increasing within-community variation in NSC also suggests a role for microsite filtering of key nutrient controls. Nonetheless, competing explanations may have more to do with climate: NSC (particularly sugars) in extracellular fluid reduces the freezing point of intracellular leaf components similar to antifreeze (Thomashow, 1999). Tropical trees may store more NSC at higher elevations (Beck, 1994), which may be particularly useful above *c.* 2000 m asl at night. Resolving linkages among NSC, temperature and other factors such as nutrient availability will require *in situ* experimental manipulations along tropical elevation gradients. Remote sensing of forest canopy NSC will be particularly helpful in locating contrasting sites for field and laboratory studies.

With increasing elevation, we observed a general increase in the distributional variance of most foliar traits (Fig. 5). Because precipitation and solar radiation do not systematically change with elevation on our gradient, increasing trait variance may be mostly driven by decreasing temperatures. Lower temperatures, and perhaps spatially and temporally variable freezing conditions at high elevations, may beget variation in foliar traits, such as LMA, among coexisting species within high-diversity communities. Changes in trait distributional variances were conspicuously absent, however, for foliar P, which maintained a relatively narrow range within communities from the Amazonian lowlands to the treeline in the Andes (Fig. 5). Our measured average mass-based foliar P values of 0.11–0.18% are at the middle to the upper end of the range for humid tropical forests (Townsend *et al.*, 2007), suggesting that P is not highly limiting in our sites, as is found in forests on highly weathered soils elsewhere in the Amazon basin (Townsend *et al.*, 2002). The elevation independence of P variation on our gradient may be reflective of generally high P availability in western Amazonian and Andean forests (Quesada *et al.*, 2009), or it may indicate a lack of temperature sensitivity of rock-derived nutrients to increasing elevation (Cleveland *et al.*, 2011; Gornish & Prather, 2014). By contrast, foliar N variance increased with elevation, suggesting competition among and adaptation of species to decreasing resource availability.

We have established the strong elevation dependence of LMA, leaf water, and NSC concentrations along the study gradient. These three traits increase in both mean value and variance up the mountain; however, the pattern is much clearer when measuring these traits at whole landscape level, rather than in 1 ha plots (Fig. 5). Whether by hand-picking leaves or by remote sensing of canopies, plot-level estimates yielded noisier information on these traits. Marvin *et al.* (2014) found that 1 ha plots poorly represented their host landscapes in above-ground carbon stocks across the Andes–Amazon region, particularly at higher elevations. Our results similarly suggest that plot-based trait distributions are not always representative of landscape trait distributions. By using remote sensing at the landscape level to measure broadscale shifts in the distributions of LMA, leaf water, and NSC, it may be possible to monitor for climatic stress, particularly increasing temperatures and/or drought effects, on plant canopies. Over time with improved instrumentation and methodologies, remote sensing of LMA, leaf water, and NSC has become increasingly possible, particularly with imaging spectrometers (Roberts *et al.*, 2004; Ustin *et al.*, 2004; Asner *et al.*, 2011; Asner & Martin, 2015). This may be particularly valuable for assessing changes in forest productivity and mortality caused by increasing temperature and drought in the Amazon basin (Phillips *et al.*, 2009; Duffy *et al.*, 2015).

Despite some of the similarities observed in the mean elevation trends for traits measured with field- or remote sensing-based approaches, we found pronounced effects of sampling approach on trait distributions. These effects exceeded those expected by the averaging effect of more remotely sensed samples relative to field samples. The shape of the trait distributions changed by sampling approach as well as by sampling grain size and extent. Sampling extent had the largest effects on trait variance and skewness, and less so on kurtosis. Distributional differences as a result of the sampling approach (field, remote sensing) and grain size (leaf level, 0.01, 1.0 ha) increased with elevation, which emphasizes the value of wide-area mapping or sampling as environmental heterogeneity increases with elevation in the Andes.

Our results also provide an opportunity to compare and contrast field and remotely sensed approaches with trait-based ecological studies. Remote sensing offers far more measurement coverage than can be achieved in the field. The economy-of-scale effect is enormous, for example, with the Carnegie Airborne Observatory routinely mapping well over 100 000 ha of forest each day at 1 m spatial resolution. For our study, *c.* 8 months were spent by technicians in the field to collect foliar samples, followed by another 8 months in the laboratory to complete chemical assays. By contrast, the airborne data acquisition, processing and conversion to chemical and LMA estimates will be just days of effort in the future, given that the approach has now been developed for operational use in the western Amazon. However, doing so requires that the airborne laboratory be deployed to the region, which takes financial, technological and logistical capacity.

An important way to advance the role of remote sensing for canopy foliar trait studies is by taking high-fidelity imaging spectrometers from their current airborne vantage points to low-Earth orbit. The only civilian imaging spectrometer to achieve orbit is Hyperion, onboard the Earth Observing-1 satellite (Ungar *et al.*, 2003). However, Hyperion is a low-fidelity imaging spectrometer that has proved difficult for use in the types of chemical estimates reported in our paper (e.g. Townsend & Foster, 2002; Smith *et al.*, 2003). The German EnMAP mission is moving forward for a 2018 launch with a spatial resolution of 30 m or 0.1 ha (Stuffler *et al.*, 2009), and could be sufficient to achieve some of the measurements demonstrated here. NASA also has plans for the HyspIRI satellite mission sometime after 2020 (Lee *et al.*, 2015), which could provide high-fidelity spectroscopy at 30–60 m (0.1–0.2 ha) resolution. Perhaps in the future, mapping of canopy foliar traits and their distributions will be routine from Earth orbit. Mapping and monitoring of changes in plant canopy traits, and their distributions, are key to understanding biospheric responses to climatic events such as drought, as well as longer-term changes in climate conditions (Schimel *et al.*, 2013). Furthermore, changes in the geographic distribution of plant canopy functional traits may be key indicators of changing biological diversity at landscape to global scales (Jetz *et al.*, 2016). Making plant functional trait mapping and monitoring routine from Earth orbit would greatly enhance our understanding of our rapidly changing planet.

Acknowledgements

This work is a product of the Andes Biodiversity and Ecosystems Research Group ABERG (http://andesresearch.org), the Global Ecosystems Monitoring (GEM) network (http://gem.tropicalforests.ox.ac.uk), the Amazon Forest Inventory Network RAINFOR (http://www.rain for.org), and the Carnegie Spectranomics Project (http://spectranomics.ciw.edu) research consortia. The field campaign was funded by a grant to Y.M. from the UK Natural Environment Research Council (grant NE/J023418/1), with additional support from European Research Council advanced investigator grants GEM-TRAITS (321131) and T-FORCES (291585), and a John D. and Catherine T. MacArthur Foundation grant to G.P.A. We thank the Servicio Nacional de Áreas Naturales Protegidas por el Estado (SERNANP) and personnel of Manu and Tambopata National Parks for logistical assistance and permission to work in the protected areas. We also thank the Explorers' Inn and the Pontifical Catholic University of Peru, as well as ACCA for use of the Tambopata and Wayqecha Research Stations, respectively. We thank E. Cosio (Pontifical Catholic University of Peru) for assistance with research permissions and sample analysis and storage. G.P.A. and the Spectranomics team were supported by the endowment of the Carnegie Institution for Science and a grant from the National Science Foundation (DEB-1146206). Y.M. was also supported by the Jackson Foundation. Carnegie Airborne Observatory data collection, processing and analyses were funded by the John D. and Catherine T. MacArthur Foundation. Use of the Carnegie Airborne Observatory was supported by the Avatar Alliance Foundation, John D. and Catherine T. MacArthur Foundation, Gordon and Betty Moore Foundation, Mary Anne Nyburg Baker and G. Leonard Baker Jr, and William R. Hearst III.

Author contributions

G.P.A., S.D., B.E. and Y.M. conceived and designed the study. G.P.A., R.E.M., C.B.A., D.E.K. and N.V. carried out the remote sensing data collection, processing and analyses. R.E.M., K.K., L.P.B., A.S., N.S., F.S., R.T., K.Q.H., M.M.P., F.D.C.Á. and Y.M. collected field data. R.E.M. and K.K. carried out laboratory assays. G.P.A., R.E.M. and C.B.A. completed integrated data analyses. G.P.A., R.E.M., B.E. and Y.M. wrote the paper.

References

Agrawal AA. 2007. Macroevolution of plant defense strategies. *Trends in Ecology and Evolution* **22**: 103–109.

Asner GP, Anderson C, Martin RE, Knapp DE, Tupayachi R, Kennedy-Bowdoin T, Sinca F, Malhi Y. 2014a. Landscape-scale changes in forest structure and functional traits along an Andes-to-Amazon elevation gradient. *Biogeosciences* **11**: 843–856.

Asner GP, Anderson CB, Martin RE, Tupayachi R, Knapp DE, Sinca F. 2015a. Landscape biogeochemistry reflected in shifting distributions of chemical traits in the Amazon forest canopy. *Nature Geoscience* **8**: 567–573.

Asner GP, Knapp DE, Boardman J, Green RO, Kennedy-Bowdoin T, Eastwood M, Martin RE, Anderson C, Field CB. 2012. Carnegie Airborne Observatory-2: increasing science data dimensionality via high-fidelity multi-sensor fusion. *Remote Sensing of Environment* **124**: 454–465.

Asner GP, Knapp DE, Kennedy-Bowdoin T, Jones MO, Martin RE, Boardman J, Field CB. 2007. Carnegie Airborne Observatory: in-flight fusion of hyperspectral imaging and waveform light detection and ranging for three-dimensional studies of ecosystems. *Journal of Applied Remote Sensing* **1**: 013536.

Asner GP, Martin RE. 2015. Spectroscopic remote sensing of non-structural carbohydrates in forest canopies. *Remote Sensing* **7**: 3526–3547.

Asner GP, Martin RE. 2016. Convergent elevation trends in canopy chemical traits of tropical forests. *Global Change Biology* **22**: 2216–2227.

Asner GP, Martin RE, Anderson CB, Knapp DE. 2015b. Quantifying forest canopy traits: imaging spectroscopy versus field survey. *Remote Sensing of Environment* **158**: 15–27.

Asner GP, Martin RE, Tupayachi R, Anderson CB, Sinca F, Carranza-Jimenez L, Martinez P. 2014b. Amazonian functional diversity from forest canopy chemical assembly. *Proceedings of the National Academy of Sciences, USA* **111**: 5604–5609.

Asner GP, Martin RE, Tupayachi R, Emerson R, Martinez P, Sinca F, Powell GVN, Wright SJ, Lugo AE. 2011. Taxonomy and remote sensing of leaf mass per area (LMA) in humid tropical forests. *Ecological Applications* **21**: 85–98.

Beck E. 1994. Cold tolerance in tropical alpine plants. In: Rundel PW, Smith AP, Meinzer C, eds. *Tropical alpine environments: plant form and function.* Cambridge, UK: Cambridge University Press, 77–110.

Boulesteix A-L, Strimmer K. 2006. Partial least squares: a versatile tool for the analysis of high-dimensional genomic data. *Briefings in Bioinformatics* **8**: 32–44.

Chen S, Hong X, Harris CJ, Sharkey PM. 2004. Sparse modeling using orthogonal forest regression with PRESS statistic and regularization. *IEEE Transaction on Systems, Man and Cybernetics* **34**: 898–911.

Cleveland CC, Townsend AR, Taylor P, Alvarez-Clare S, Bustamante MMC, Chuyong G, Dobrowski SZ, Grierson P, Harms KE, Houlton BZ *et al.* 2011. Relationships among net primary productivity, nutrients and climate in tropical rain forest: a pan-tropical analysis. *Ecology Letters* **14**: 939–947.

Colgan MS, Baldeck CA, Féret J-B, Asner GP. 2012. Mapping savanna tree species at ecosystem scales using support vector machine classification and

BRDF correction on airborne hyperspectral and LiDAR data. *Remote Sensing* **4**: 3462–3480.

Cordell S, Goldstein G, Mueller-Dombois D, Webb D, Vitousek PM. 1998. Physiological and morphological variation in *Metrosideros polymorpha*, a dominant Hawaiian tree species, along an altitudinal gradient: the role of phenotypic plasticity. *Oecologia* **113**: 188–196.

Cornelissen JHC, Lavorel S, Garnier E, Diaz S, Buchmann N, Gurvich DE, Reich PB, Ter Steege H, Morgan HD, Van Der Heijden MGA. 2003. A handbook of protocols for standardised and easy measurement of plant functional traits worldwide. *Australian Journal of Botany* **51**: 335–380.

Cornwell WK, Ackerly DD. 2009. Community assembly and shifts in plant trait distributions across an environmental gradient in coastal California. *Ecological Monographs* **79**: 109–126.

Demarty M, Morvan C, Thellier M. 1984. Calcium and the cell wall. *Plant, Cell & Environment* **7**: 441–448.

Dietze MC, Sala A, Carbone MS, Czimczik CI, Mantooth JA, Richardson AD, Vargas R. 2014. Nonstructural carbon in woody plants. *Annual Review of Plant Biology* **65**: 667–687.

Duffy PB, Brando P, Asner GP, Field CB. 2015. Projections of future meteorological drought and wet periods in the Amazon. *Proceedings of the National Academy of Sciences, USA* **112**: 13172–13177.

Feilhauer H, Asner GP, Martin RE, Schmidtlein S. 2010. Brightness-normalized partial least squares regression for hyperspectral data. *Journal of Quantitative Spectroscopy and Radiative Transfer* **111**: 1947–1957.

Fisher J, Malhi Y, Torres I, Metcalfe D, van de Weg M, Meir P, Silva-Espejo J, Huasco W. 2013. Nutrient limitation in rainforests and cloud forests along a 3,000-m elevation gradient in the Peruvian Andes. *Oecologia* **172**: 889–902.

Gentry AH. 1988. Changes in plant community diversity and floristic composition on environmental and geographical gradients. *Annals of the Missouri Botanical Garden* **75**: 1–34.

Gilliham M, Dayod M, Hocking BJ, Xu B, Conn SJ, Kaiser BN, Leigh RA, Tyerman SD. 2011. Calcium delivery and storage in plant leaves: exploring the link with water flow. *Journal of Experimental Botany* **62**: 2233–2250.

Girardin CAJ, Farfan-Rios W, Garcia K, Feeley KJ, Jorgensen PM, Murakami AA, Cayola Perez L, Seidel R, Paniagua N, Fuentes Claros AF *et al.* 2013. Spatial patterns of above-ground structure, biomass and composition in a network of six Andean elevation transects. *Plant Ecology & Diversity* **7**: 161–171.

Gornish ES, Prather CM. 2014. Foliar functional traits that predict plant biomass response to warming. *Journal of Vegetation Science* **25**: 919–927.

Haaland DM, Thomas EV. 1988. Partial least-squares methods for spectral Analyses. 1. Relation to other quantitative calibration methods and the extraction of qualitative information. *Analytical Chemistry* **60**: 1193–1202.

Hikosaka K, Nagamatsu D, Ishii HS, Hirose T. 2002. Photosynthesis-nitrogen relationships in species at different altitudes on Mount Kinabalu, Malaysia. *Ecological Research* **17**: 305–313.

von Humboldt A. 1850. *Aspects of nature in different lands and different climates.* Philadelphia, PA, USA: Lea and Blanchard.

Jetz W, Cavender-Bares J, Pavlick R, Schimel D, Davis FW, Asner GP, Guralnick R, Kattge J, Latimer AM, Moorcroft P. 2016. Monitoring plant functional diversity from space. *Nature Plants* **2**: 16024.

Kokaly RF, Asner GP, Ollinger SV, Martin ME, Wessman CA. 2009. Characterizing canopy biochemistry from imaging spectroscopy and its application to ecosystem studies. *Remote Sensing of Environment* **113**: S78–S91.

Körner C, Bannister P, Mark AF. 1986. Altitudinal variation in stomatal conductance, nitrogen content and leaf anatomy in different plant life forms in New Zealand. *Oecologia* **69**: 577–588.

Körner C, Farquhar GD, Roskandic Z. 1988. A global survey of carbon isotope discrimination in plants from high altitude. *Oecologia* **74**: 623–632.

Kruse FA, Lefkoff AB, Boardman JB, Heidebrecht KB, Shapiro AT, Barloon PJ, Goetz AFH. 1993. The Spectral Image Processing System (SIPS) – interactive visualization and analysis of imaging spectrometer data. *Remote Sensing of Environment* **44**: 145–163.

Lee CM, Cable ML, Hook SJ, Green RO, Ustin SL, Mandl DJ, Middleton EM. 2015. An introduction to the NASA Hyperspectral InfraRed Imager (HyspIRI) mission and preparatory activities. *Remote Sensing of Environment* **167**: 6–19.

Malhi Y, Silman M, Salinas N, Bush M, Meir P, Saatchi S. 2010. Introduction: elevation gradients in the tropics: laboratories for ecosystem ecology and global change research. *Global Change Biology* **16**: 3171–3175.

Martens H. 2001. Reliable and relevant modelling of real world data: a personal account of the development of PLS Regression. *Chemometrics and Intelligent Laboratory Systems* **58**: 85–95.

Marvin DC, Asner GP, Knapp DE, Anderson CB, Martin RE, Sinca F, Tupayachi R. 2014. Amazonian landscapes and the bias in field studies of forest structure and biomass. *Proceedings of the National Academy of Sciences, USA* **111**: E5224–E5232.

Metcalfe DB, Asner GP, Martin RE, Silva Espejo JE, Huasco WH, Farfán Amézquita FF, Carranza-Jimenez L, Galiano Cabrera DF, Baca LD, Sinca F *et al.* 2014. Herbivory makes major contributions to ecosystem carbon and nutrient cycling in tropical forests. *Ecology Letters* **17**: 324–332.

Myneni RB, Ross J, Asrar G. 1989. A review on the theory of photon transport in leaf canopies. *Agricultural and Forest Meteorology* **45**: 1–153.

Nottingham AT, Ccahuana AJQ, Meir P. 2012. Soil properties in tropical montane cloud forests influence estimates of soil CO_2 efflux. *Agricultural and Forest Meteorology* **166**(167): 215–220.

Phillips OL, Aragao LEOC, Lewis SL, Fisher JB, Lloyd J, Lopez-Gonzalez G, Malhi Y, Monteagudo A, Peacock J, Quesada CA *et al.* 2009. Drought Sensitivity of the Amazon Rainforest. *Science* **323**: 1344–1347.

Poorter H, Niinemets U, Poorter L, Wright IJ, Villar R. 2009. Causes and consequences of variation in leaf mass per area (LMA): a meta-analysis. *New Phytologist* **182**: 565–588.

Quentin AG, Pinkard EA, Ryan MG, Tissue DT, Baggett LS, Adams HD, Maillard P, Marchand J, Landheusser SM, Lacointe A. 2015. Non-structural carbohydrates in woody plants compared among laboratories. *Tree Physiology* **35**: 1146–1165.

Quesada C, Lloyd J, Schwarz M, Baker T, Phillips O, Patiño S, Czimczik C, Hodnett M, Herrera R, Arneth A. 2009. Regional and large-scale patterns in Amazon forest structure and function are mediated by variations in soil physical and chemical properties. *Biogeosciences* **6**: 3993–4057.

Roberts DA, Ustin SL, Ogunjemiyo S, Greenberg J, Dobrowski SZ, Chen JQ, Hinckley TM. 2004. Spectral and structural measures of northwest forest vegetation at leaf to landscape scales. *Ecosystems* **7**: 545–562.

Roderick ML, Berry SL, Noble IR. 2000. A framework for understanding the relationship between environment and vegetation based on the surface area to volume ratio of leaves. *Functional Ecology* **14**: 423–437.

Sakschewski B, von Bloh W, Boit A, Rammig A, Kattge J, Poorter L, Peualeas J, Wright IJ, Thonicke K. 2015. Leaf and stem economics spectra drive functional diversity in a dynamic global vegetation model. *Global Change Biology* **21**: 2711–2725.

Schimel DS, Asner GP, Moorcroft PR. 2013. Observing changing ecological diversity in the Anthropocene. *Frontiers in Ecology and the Environment* **11**: 129–137.

Schlesinger WH. 1991. *Biogeochemistry, an analysis of global change.* San Diego, CA, USA: Academic Press.

Schuur EAG, Matson PA. 2001. Net primary productivity and nutrient cycling across a mesic to wet precipitation gradient in Hawaiian montane forest. *Oecologia* **128**: 431–442.

Sides CB, Enquist BJ, Ebersole JJ, Smith MN, Henderson AN, Sloat LL. 2014. Revisiting Darwin's hypothesis: does greater intraspecific variability increase species' ecological breadth? *American Journal of Botany* **101**: 56–62.

Smith ML, Martin ME, Plourde L, Ollinger SV. 2003. Analysis of hyperspectral data for estimation of temperate forest canopy nitrogen concentration: comparison between airborne (AVIRIS) and spaceborne (Hyperion) sensor. *IEEE Transaction of Geoscience and Remote Sensing* **41**: 1332–1337.

Stuffler T, Förster K, Hofer S, Leipold M, Sang B, Kaufmann H, Penné B, Mueller A, Chlebek C. 2009. Hyperspectral imaging: an advanced instrument concept for the EnMAP mission (Environmental Mapping and Analysis Programme). *Acta Astronautica* **65**: 1107–1112.

Thomashow MF. 1999. Plant cold acclimation: freezing tolerance genes and regulatory mechanisms. *Annual Review of Plant Physiology and Plant Molecular Biology* **50**: 571–599.

Townsend AR, Asner GP, Cleveland CC. 2008. The biogeochemical heterogeneity of tropical forests. *Trends in Ecology and the Environment* **23**: 424–431.

Townsend AR, Asner GP, Cleveland CC, Lefer ME, Bustamante MMC. 2002. Unexpected changes in soil phosphorus dynamics along pasture chronosequences in the humid tropics. *Journal of Geophysical Research-Atmospheres* **107**: 8067.

Townsend AR, Cleveland CC, Asner GP, Bustamante MMC. 2007. Controls over foliar N: P ratios in tropical rain forests. *Ecology* **88**: 107–118.

Townsend PA, Foster JR. 2002. Comparison of EO-1 Hyperion to AVIRIS for mapping forest composition in the Appalachian Mountains, USA. *International Geoscience and Remote Sensing Symposium (IGARSS)* **2**: 793.

Ungar SG, Pearlman JS, Mendenhall JA, Reuter D. 2003. Overview of the Earth Observing One (EO-1) mission. *IEEE Transactions on Geoscience and Remote Sensing* **41**: 1149–1160.

Ustin SL, Gitelson AA, Jacquemoud S, Schaepman M, Asner GP, Gamon JA, Zarco-Tejada P. 2009. Retrieval of foliar information about plant pigment systems from high resolution spectroscopy. *Remote Sensing of Environment* **113**: S67–S77.

Ustin SL, Roberts DA, Gamon JA, Asner GP, Green RO. 2004. Using imaging spectroscopy to study ecosystem processes and properties. *BioScience* **54**: 523–534.

Vitousek P. 1982. Nutrient cycling and nutrient use efficiency. *American Naturalist* **119**: 553–572.

Westoby M, Wright IJ. 2006. Land-plant ecology on the basis of functional traits. *Trends in Ecology & Evolution* **21**: 261–268.

Wright IJ, Reich PB, Westoby M. 2001. Strategy shifts in leaf physiology, structure and nutrient content between species of high- and low-rainfall and high- and low-nutrient habitats. *Functional Ecology* **15**: 423–434.

Supporting Information

Additional Supporting Information may be found online in the Supporting Information tab for this article:

Fig. S1 Changes in average leaf nitrogen (N) per unit leaf area with increasing elevation along the Andes–Amazon study gradient.

Table S1 Community-mean trait values generated from field-based leaf collections using different averaging methods

Table S2 Multiple linear regression model *F*-statistics relating canopy foliar trait statistics and elevation using three field-based sample analysis approaches

Table S3 Site-level statistical results for leaf collections in 1.0 ha plots

Please note: Wiley Blackwell are not responsible for the content or functionality of any supporting information supplied by the authors. Any queries (other than missing material) should be directed to the *New Phytologist* Central Office.